EURASIP Journal on Advances in Signal Processing
a SpringerOpen Journal

RESEARCH Open Access

Low-complexity iterative receiver design for mobile OFDM systems

Vamadevan Namboodiri[1,2*], Hong Liu[2] and Predrag Spasojević[1]

Abstract

Iterative receivers with minimum mean square error turbo equalization are computationally involved, as they require some form of matrix inversion. In this article, we propose a low complexity iterative receiver that implements successive interference cancelation-based MAP decoding (SIC-MAP) in doubly dispersive channels for orthogonal frequency division multiplexing systems. SIC-MAP leverages the soft feedback symbol estimates to remove the intercarrier interference from the received data. Numerical simulation results show that the proposed scheme achieves BER performance comparable to that of the equalization schemes proposed in Schniter et al. and Fang et al. but with significant computational savings. A low-complexity least squares-based iterative channel estimation scheme using soft feedback information is also proposed. This scheme is especially suitable when the number of significant channel taps is higher than the number of pilots, a phenomenon that is encountered by receivers in Single Frequency Networks (for example, DVB deployments in Europe).

Introduction

Orthogonal frequency division multiplexing (OFDM)-based systems have been adopted in many of the recent wireless communication standards, such as European terrestrial broadcast systems based on DVB-H, DVB-T, and DVB-T2, and cellular wireless communication systems based on 4G. For OFDM systems, a cyclic prefix (CP) of sufficient length makes the receiver design simple (1-tap equalizer) in frequency-selective multipath environments. Modern wireless communications applications, however, require high data rates at high carrier frequencies and at high levels of mobility. Addressing these requirements results in less intercarrier spacing and severe time-varying frequency-selective multipath fading. These outcomes break the orthogonality of subcarriers and lead to intercarrier interference (ICI), thus severely impacting the receiver BER performance. In DVB-H, for example, the intercarrier spacing (ICS) could be as low as approximately 1 kHz, and the expected maximum receiver Doppler frequency is of the order of 10–20% of the ICS. In such scenarios, efficient receiver design is a challenging practical problem.

The vast majority of schemes proposed in the literature to cope with the issue described above fall into three categories: (a) independent equalization and decoding [1-4]. In [4], the received signal is split into small segments such that the channels remain approximately static during each small segment. Suitable signal processing is performed on each of these segments, such that the resulting channel matrix is made diagonal. Consequently, the equalizer becomes single tap. To mitigate the ICI in large-sized symbol systems such as DVB-T2, [2] proposes using a pre-equalizer. At first, the symbol is divided into smaller sizes. A pre-equalizer based on minimizing the ICI power is implemented, followed by a single-tap equalizer to compensate for channel selectivity. The authors of [1] propose a minimum mean square error (MMSE) filter that takes not only the subcarrier amplitudes but also their derivatives, to compute the transmitted symbol estimate. In [3], an iterative decision feedback equalizer (DFE) is proposed to perform ICI cancelation such that the modified system matrix becomes diagonal in the frequency domain. (b) Successive cancelation of the interference [5-8]. In [5], ICI is removed in the time domain. The signal is then converted to the frequency domain, thus resulting in a diagonal frequency domain system matrix. Hard decisions are made on the equalized signal, after which it is converted back to the time domain, and the time-frequency

*Correspondence: vnambood@winlab.rutgers.edu
[1]WINLAB, Rutgers University, North Brunswick, NJ, USA
[2]Broadcom Corporation, Holland, PA, USA

iterations are repeated. In [6], derived for MIMO systems, a new MMSE filter taking the decision errors into account is derived. A MMSE estimate of each QAM symbol from each antenna (rather than a joint estimation of symbols from all antennas) is used successively to cancel the interference coming from other antennas. In [7], the mean value of the transmit symbol is computed using the LLR values from the decoder. The mean value is then used to remove the ICI from the received symbol, resulting in a diagonal system matrix. A modified low-complexity MMSE equalizer that takes the decision error into account is then derived. In the context of interference cancelation in CDMA systems, authors of [8] propose a MMSE estimator where the estimate of the desired signal is computed repeatedly, each time rearranging the order of interference cancelation using a novel algorithm. They then select the most likely estimate (that has the least error) from the above list. (c) Turbo-like iterative equalization [9-16]. The original turbo equalization (TE) proposed by [9] has exponential complexity. Subsequently, MMSE-based reduced complexity TE is proposed in [10,11], where the computation complexity is $O(N^3)$ or $O(N^2)$. The authors of [16] propose a modified LMMSE equalizer that provides a more accurate modeling of the statistics of the two quadrature components of the transmitted symbol. It is claimed to have better performance compared to [11]. The authors of [12] propose an iterative equalization scheme for communication systems that operate under water. It includes a channel estimation scheme for rapidly varying channels. The channel that is assumed to follow a three-parameter model is estimated using convex optimization techniques in an iterative fashion. In [13], the authors propose a low-complexity MAP decoding for doubly selective OFDM systems. The proposed algorithm successively computes the symbols and removes from the observation the interference due to these symbols, thus bringing down the search space progressively and significantly reducing the decoding complexity. The successive symbol search is made in a computationally efficient manner by making use of the Markov Chain Monte Carlo (MCMC) method with Gibbs sampling. In [14], the authors propose an OFDM MIMO detection based on successive cancelation of interference. Using a novel LLR criteria, the layers with the least MSE error are successively identified, and MMSE-based TE is then applied iteratively to estimate the symbols from the selected layer. The contributions of these estimated symbols are then subtracted from the observation before making a new MMSE estimate. In [15], an iterative technique for the inversion of a linear system of equations called "operator-perturbation technique" is used to cancel ICI iteratively. Turbo-like iterative schemes, in general, are found to have superior performance among the schemes described. The turbo schemes described above, however, are saddled, in general, with high computational complexity (quadratic or sometimes cubic in the number of subcarriers). Such practical application challenges motivate us to come up with a new scheme with a better trade-off between performance and implementation complexity.

Encouraged by the development of MMSE-based turbo equalization schemes [10,11], a large number of low-complexity iterative OFDM equalization schemes have been proposed [17-19]. They exploit the banded nature of the frequency domain channel matrix to bring down the equalization complexity to linear with the number of subcarriers. The references above propose, in general, either a new technique for iterative MMSE linear equalization using priors on the banded submatrix around the main diagonal, or a new technique to compute the soft information from the symbol estimates.

Although the joint processing of equalization and decoding is the most optimal solution, it is computationally expensive and, thus, not viable in practical receivers. In this article, we propose a suboptimal, successive interference cancelation-based MAP decoder, wherein we avoid the explicit equalization stage. In SIC-MAP, we keep the contributions from the same transmit symbol on consecutive received symbols while eliminating the interference from the other transmit symbols, which are estimated using the feedback information from the decoder. This method results in multiple receiver observations for the same transmit symbol, as in the case of a diversity system. The resulting system matrix becomes a single-column matrix. It is easy to implement MAP decoding in such systems. As in references [18-20], we also exploit the banded nature of the system matrix in SIC-MAP. The performance and computational complexity of the proposed scheme is compared with that of MMSE-TE-OND2, suggested in [18], and TE-BLK2, the best performing equalizer in a group of three [19]. In [18,19], a windowing technique is used to make the energy more concentrated along the diagonal. The windowing mentioned in those articles will also work in our proposed scheme. We incorporate channel coding in [18,19] to render a fair comparison. It has been found that SIC-MAP provides a comparable performance to MMSE-TE-OND2 and TE-BLK2 but with significantly less computational complexity. Such a receiver, compared to their counterparts, will take only a fraction of the silicon area (or the cost) and battery power, a scarce resource in mobile applications, thus making it especially suitable for mobile applications with large symbol lengths, such as [21,22].

Accurate estimating of channel state information (CSI) is essential for the effectiveness of any equalization/decoding scheme. Examples of such schemes include techniques using singular value decomposition (SVD) [23]. Inspired by the channel estimation algorithm proposed in [5], we propose a soft decision feedback-based

low-cost least squares (LS) estimation scheme. The proposed algorithm makes use of soft information to refine the channel estimates so that they are capable of handling the long channel scenarios, such as those encountered in Single Frequency Networks (SFN) (for example, DVB deployment in Europe). In such networks, the number of significant channel taps can be higher than the number of pilot subcarriers.

This article is organized as follows: notations used in this article are explained first. In **System model** section, the system model is presented, following which we describe SIC-MAP in **Successive interference cancelation-based MAP receiver (SIC-MAP)** section. In **Channel estimation** section , we present a low-complexity channel estimation scheme suitable for this equalizer. In **The proposed IR with SIC-MAP** section, the overall algorithm is presented, and in **Computational complexity analysis** section, we compare the computational complexity of SIC-MAP with similar equalization schemes. In **Numerical results and discussion** section, the numerical results are presented. In **Conclusion** section, we draw the final conclusions

Notation: $(\cdot)^t$ denotes transpose, $(\cdot)^H$ conjugate transpose (Hermitian), $\{a\}$ denotes a set with elements $\{a(0), a(1), ..\}$, $\mathbf{F}$ for normalized N point Discrete Fourier Transform (DFT), where $\mathbf{F}_{k,l} := (1/\sqrt{N})e^{-j2\pi kl/N}$, $\mathbf{I}$ is the identity matrix, $\mathbf{i}_k$ is the k^{th} column of $\mathbf{I}$, $||\cdot||$ for l_2-norm, $\lceil\cdot\rceil$ is the ceiling of a function, $Re(\cdot)$ and $Im(\cdot)$ for the real and imaginary parts of a complex quantity. $diag(\boldsymbol{\nu}_x)$ is the diagonal matrix from the vector $\boldsymbol{\nu}_x$. Expectation is denoted by $E\{\cdot\}$. Bold lowercase letters, e.g., $\mathbf{x}$, denote vectors, and bold uppercase letters, e.g., $\mathbf{X}$, denote matrices.

System model

The OFDM transceiver model is described in Figure 1. At the transmitter, information bits ($\{a(n)\}$) are convolutionally encoded ($\{b(n)\}$) and passed through a bit interleaver (BI) ($\{c(n)\}$). The symbol mapper modulates them into QAM symbols ($\{s(k)\}$). A set of N of these QAM "frequency domain" symbols is collected to form an OFDM symbol. A symbol interleaver (SI) interleaves them ($\mathbf{x}$). The OFDM symbol is converted into "discrete time-domain" samples, $\{z(i)\}$, by performing an N point IDFT. A cyclic prefix (CP) of length $N_p \leq N$ is added to each of these symbols. These samples are then transmitted from the transmit antenna. The multipath channel is modeled as a linear time-varying (LTV) system with discrete impulse response $h(i,l)$ (time i response to an impulse at time $i-l$ for the wireless channel). At the receiver, the CP removed data is converted back to the "frequency domain" by performing an N point DFT and is passed to the symbol Detection-Decoding block. It comprises Successive Interference Canceler (SIC), Channel Estimator, Symbol and Bit Interleaver/de-interleaver, Log Likelihood Ratio (LLR) Computer and BCJR- or SOVA-based decoder [24].

We assume perfect carrier, symbol and sample synchronization at the receiver. Given that maximum channel taps $N_h \leq N_p$, the received samples in the base band can be represented as,

$$r(i) = \sum_{l=0}^{N_h-1} h(i,l)z(i-l) + n(i), 0 \leq i < N, \tag{1}$$

where $\{n(i)\}$ are samples of additive white Gaussian noise (AWGN) with zero mean and variance σ^2. Defining $\mathbf{r} := [r(0), r(1), \ldots, r(N-1)]^t$, the received vector corresponding to a single OFDM symbol, $\mathbf{r}$, can be written as follows:

$$\mathbf{r} = \boldsymbol{\Xi}\mathbf{z} + \boldsymbol{\psi} \tag{2}$$

$$\boldsymbol{\Xi} := \begin{bmatrix} h(0,0) & \ldots & h(0,N_h-1) & \ldots & h(0,1) \\ h(1,1) & h(1,0) & \ldots & \ldots & h(1,2) \\ \ldots & \ldots & \ldots & \ldots & \ldots \\ 0 & \ldots & h(N-1,N_h-1) & \ldots & h(N-1,0) \end{bmatrix} \tag{3}$$

where $\boldsymbol{\Xi}$ is the time varying system matrix determined by the channel estimator and is given in (3), and $\boldsymbol{\psi} := [n(0), n(1), \cdots, n(N-1)]^t$. CP is removed from these "time domain" samples. N such samples are grouped together and presented to a DFT processor, which, in turn, outputs N "frequency domain" samples, $\{y(k)\}$. Taking a DFT on both sides of (2),

$$\begin{aligned} \mathbf{y} = \mathbf{F}\mathbf{r} &= \mathbf{F}\boldsymbol{\Xi}\mathbf{F}^H\mathbf{x} + \mathbf{w} \\ &= \mathbf{H}\mathbf{x} + \mathbf{w} \end{aligned} \tag{4}$$

where $\mathbf{H} := \mathbf{F}\boldsymbol{\Xi}\mathbf{F}^H$, $\mathbf{y} := [y(0), y(1), \cdots, y(N-1)]^t$, $\mathbf{x} := [x(0), x(1), \cdots, x(N-1)]^t$ and $\mathbf{w} = \mathbf{F}\boldsymbol{\psi}$. Note that $\mathbf{w}$ is wide sense stationary (WSS), with the same mean and covariance as that of $\boldsymbol{\psi}$, as $\mathbf{F}$ is unitary. Here, $\mathbf{x}$ is the transmitted OFDM symbol, $\mathbf{H}$ is the channel matrix in the frequency domain and $\mathbf{y}$ is the received OFDM symbol. If the channel is static, $\mathbf{H}$ will be a diagonal matrix. In the case of time-varying Rayleigh fading channels [25], it has been shown that $\mathbf{H}$ will be a banded matrix with significant coefficients concentrated in a banded structure, with width D along the diagonal. D is typically chosen as $D = 2L+1$, where $L = \lceil f_d T_s N \rceil$, f_d is the normalized maximum Doppler frequency and T_s is the sample duration. Different structures for $\mathbf{H}$ are shown in Figure 2 [18].

Successive interference cancelation-based MAP receiver (SIC-MAP)

In this section, we present a low-complexity IR that implements successive interference cancelation, followed by maximum *a posteriori* probability (MAP) decoding. The proposed scheme, at first, simplifies the system matrix to a

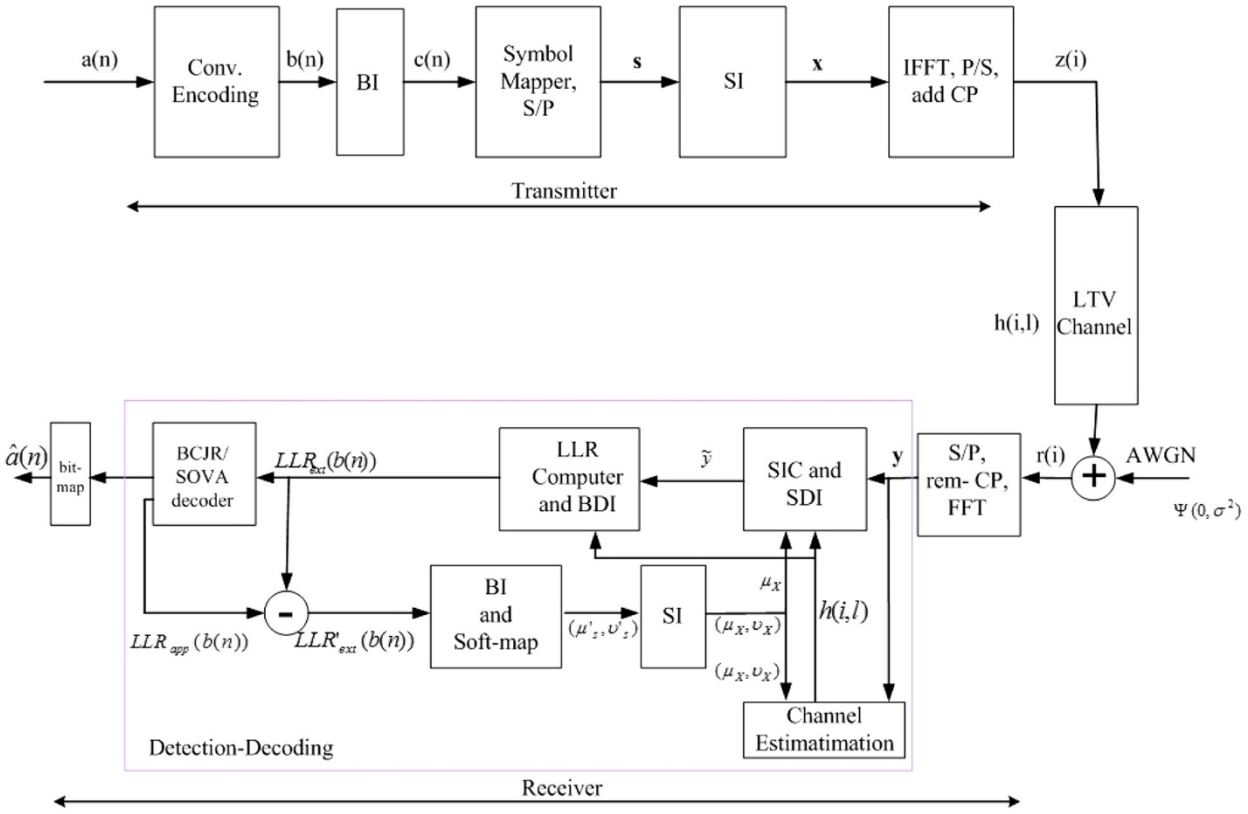

Figure 1 OFDM transceiver.

single column vector by selectively removing the ICI interference from the received symbols, using the feedback symbol mean values. Soft information can be computed directly with low cost from this modified model. This information is fed to a MAP bit decoder.

The following observations are key in formulating the proposed scheme:

1. The relative magnitude of each subdiagonal and superdiagonal element of the doubly selective Rayleigh fading channel matrix **H** decreases significantly as we move away from the main diagonal. We can, thus, ignore all elements that are far away from the main diagonal [18-20] without significantly impacting performance. Note that these elements are absent for a static multipath channel.
2. As the *extrinsic* information becomes more accurate over multiple iterations, the conditional mean, $\mu_x(k) \rightarrow x(k)$, which is the true symbol value and the conditional variance, $\upsilon_x(k) \rightarrow 0$.

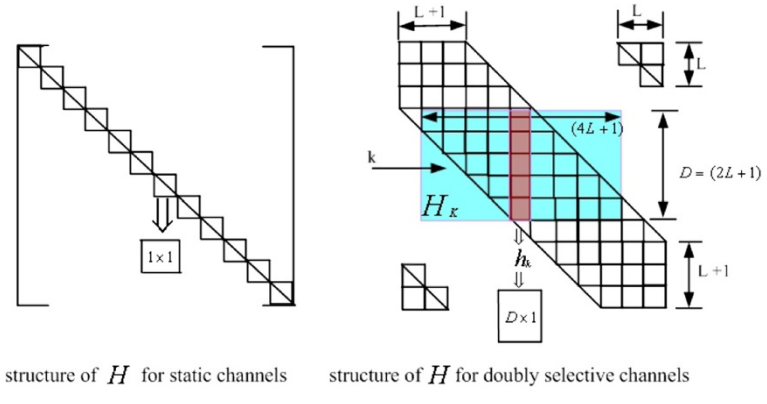

Figure 2 OFDM channel structure.

Therefore, in each new iteration, we can use $\mu_x(k)$ from the previous iteration to selectively remove ICI from the received symbol, such that the resulting system matrix is turned into a single-column vector. We compute the log likelihood ratios (LLR) $(ln\left(\frac{P(b(n)=0)}{P(b(n)=1)}\right))$ from the modified system directly, thus avoiding MMSE symbol estimation and the associated matrix inversion.

Based on observation 1, ((4)) can be approximated as

$$\begin{aligned}\mathbf{y_k} &:= [y(\langle k-L\rangle_N),\cdots,y(\langle k+L\rangle_N)]^t \\ &= \mathbf{H_k x_k} + \mathbf{w_k}\end{aligned} \tag{5}$$

where $\mathbf{x_k} := [x(\langle k-2L\rangle_N),\cdots,x(\langle k+2L\rangle_N)]^t$, $\mathbf{w_k} := [w(\langle k-L\rangle_N),\cdots,w(\langle k+L\rangle_N)]^t$ and $\mathbf{H_k}$ is the shaded (green) section of $\mathbf{H}$ in Figure 2 (right) given by (6). For simplicity of notation, the modulo operation ($\langle\rangle_N$) is omitted in the sequel.

$$\mathbf{H_k} := \begin{bmatrix} h(\langle k-L\rangle_N,\langle k-2L\rangle_N) & \dots & h(\langle k-L\rangle_N,\langle k+2L\rangle_N) \\ h(\langle k-L+1\rangle_N,\langle k-2L\rangle_N) & \dots & h(\langle k-L+1\rangle_N,\langle k+2L\rangle_N) \\ \dots & \dots & \dots \\ h(\langle k+L\rangle_N,\langle k-2L\rangle_N) & \dots & h(\langle k+L\rangle_N,\langle k+2L\rangle_N) \end{bmatrix} \tag{6}$$

Now, $\mathbf{x_k} = \boldsymbol{\mu}_{\mathbf{x_k}} + \boldsymbol{\delta}_{\mathbf{x_k}}$ where $\boldsymbol{\delta}_{\mathbf{x_k}}$ is the residual error, which approaches $\mathbf{0}_{4L+1}$ as the extrinsic LLR becomes more reliable over multiple iterations. Substituting for $\mathbf{x_k}$ in (5) and rearranging yields (7). The new noise, $\tilde{\mathbf{w}}_\mathbf{k}$, contains the ICI from the residual error $\delta_{\mathbf{x_k}}$. $\tilde{\mu}_{\mathbf{x_k}}$ is a vector as defined in (7).

$$\mathbf{y_k} = \mathbf{h_k}x(k) + \mathbf{H_k}\underbrace{\begin{bmatrix}\mu_x(k-2L)\\ \vdots \\ 0 \\ \vdots \\ \mu_x(k+2L)\end{bmatrix}}_{\tilde{\mu}_{\mathbf{x_k}}} + \mathbf{H_k}\underbrace{\begin{bmatrix}\delta_x(k-2L)\\ \vdots \\ \mathbf{0} \\ \vdots \\ \delta_x(k+2L)\end{bmatrix}}_{\tilde{\mathbf{w}}_\mathbf{k}} + \mathbf{w_k} \tag{7}$$

Let

$$\begin{aligned}\tilde{\mathbf{y}}_k &:= \mathbf{y_k} - \mathbf{H_k}\tilde{\boldsymbol{\mu}}_{\mathbf{x_k}} \\ &= \mathbf{h_k}x(k) + \tilde{\mathbf{w}}_\mathbf{k}.\end{aligned} \tag{8}$$

$\mathbf{h_k}$ is shown in red in Figure 2 (right). It is a column vector of size $D \times 1$. We also approximate that $\tilde{\mathbf{w}}_\mathbf{k}$ and $\mathbf{w_k}$ have identical covariance, as the noise due to residual ICI is small and decreasing over multiple iterations.

The LLR computer calculates the *extrinsic* LLR, $LLR_{\text{ext}}(c(n))$, which represents information about $c(n)$ contained in $\tilde{\mathbf{y}}_k$ and $P(c(l))$ for all $l \neq n$. These are passed to a MAP decoder where they are used as *a priory* LLRs. Using (9), $LLR_{\text{ext}}(c(n))$ is calculated from the modified system, where $0 \leq u \leq Q-1$, $\mathbf{m} = [m_0, m_1, \cdot, m_{Q-1}]^t$, $\{\eta\} = map(\mathbf{m})$ is the signal constellation and F_2 is binary Galois Field. Q denotes the number of bits per symbol. For example, for BPSK $Q = 1$, for QPSK $Q = 2$, and so on.

$$\begin{aligned}LLR_{\text{ext}}(c(Qk+u)) &= LLR_{\text{app}}(c(Qk+u)) - LLR(c(Qk+u)) \\ &= ln\frac{P((c(Qk+u)=0)/\tilde{\mathbf{y}}_k)}{P((c(Qk+u)=1)/\tilde{\mathbf{y}}_k)} - LLR(c(Qk+u)) \\ &= ln\frac{p(\tilde{\mathbf{y}}_k/(c(Qk+u)=0))P(c(Qk+u)=0)}{p(\tilde{\mathbf{y}}_k/(c(Qk+u)=1))P(c(Qk+u)=1)} \\ &\quad - LLR(c(Qk+u)) \\ &= \left(ln\frac{p(\tilde{\mathbf{y}}_k/(c(Qk+u)=0))}{p(\tilde{\mathbf{y}}_k/(c(Qk+u)=1))} + LLR(c(Qk+u))\right) \\ &\quad - LLR(c(Qk+u)) \\ &= ln\frac{\sum_{\mathbf{m}\in F_2:\mathbf{m}_u=0} p(\tilde{\mathbf{y}}_k/(x(k)=map(\mathbf{m})))\prod_{j=0;j\neq u}^{Q-1}P(m_j)}{\sum_{\mathbf{m}\in F_2:\mathbf{m}_u=1} p(\tilde{\mathbf{y}}_k/(x(k)=map(\mathbf{m})))\prod_{j=0;j\neq u}^{Q-1}P(m_j)}\end{aligned} \tag{9}$$

As shown in **Appendix**, for QPSK, the above expression can be simplified as

$$LLR_{ext}(c_q(2k)) = \frac{\sqrt{8}Re(\tilde{\mathbf{y}}_\mathbf{k}^H\mathbf{h_k})}{\sigma^2} \tag{10}$$

$$LLR_{ext}(c_q(2k+1)) = \frac{\sqrt{8}Im(\tilde{\mathbf{y}}_\mathbf{k}^H\mathbf{h_k})}{\sigma^2}. \tag{11}$$

A closer look at the derivation in **Appendix** reveals that this expression is applicable, within a scale factor, to any constant-modulus constellation. Observe that the *extrinsic LLR* of $c(n)$ is conditioned only on $\tilde{\mathbf{y}}_k$ and, in the simplified system model, $\tilde{\mathbf{y}}_k$ depends only on the present symbol $x(k)$. This makes the evaluation of $LLR_{\text{ext}}(c(n))$ easy. The MAP decoder computes soft outputs, $LLR_{app}(b(n))$—the *a posteriori* reliability information of each coded bit—in LLR form by minimizing the bit error probability (BEP) [24]. The input *a priori* LLR to the decoder is subtracted from $LLR_{\text{app}}(b(n))$ to obtain the *extrinsic* reliability information $LLR'_{\text{ext}}(b(n))$. It is passed through a bit interleaver and is used in the soft-mapper to compute the mean $\boldsymbol{\mu}'_s$ and the variance $\boldsymbol{\nu}'_s$. These are symbol-interleaved to produce $\boldsymbol{\mu}_x$ and $\boldsymbol{\nu}_x$. As described in (8), $\boldsymbol{\mu}_x$ is used to remove the ICI interference, whereas $\boldsymbol{\nu}_x$ is used in the channel estimator to determine the reliability of $\boldsymbol{\mu}_x$. The ICI-removed data is fed to the LLR computer to generate more reliable LLRs to further improve the output bit estimate. This process is repeated until further gains are insignificant. $LLR_{\text{app}}(b(n))$ are then hard-sliced at the bit-map block, and information bit estimates $\hat{a}(n)$ are retrieved from the received data bit estimates $\hat{b}(n)$. The mapping of $LLR'_{\text{ext}}(c(n))$s to $\mu'_s(k)$ is described in [10].

For QPSK modulation

$$\begin{aligned}\mu'_s(k) &= \tanh(LLR'_{\text{ext}}(c(2n))/2) \\ &\quad + i\tanh(LLR'_{\text{ext}}(c(2n+1))/2),\end{aligned} \tag{12}$$

$$\nu'_s(k) = 1 - \left|\mu'_s(k)\right|^2. \tag{13}$$

Notice that the approximation in (8) may not be valid for a generic system matrix $\mathbf{H_k}$. It fits the scenario, however, of doubly selective OFDM channels, where the magnitude of the off-diagonal elements in the frequency domain is significantly smaller than that of the main-diagonal elements. This gives rise only to a relatively small residual ICI power (ICI after cancelation), even with a moderate value of $\delta_{\mathbf{x_k}}$ in the early iterations, and as the iterations proceed, the approximation becomes progressively more accurate.

Channel estimation

In this section, we propose a low-complexity channel estimation scheme in OFDM systems under severe Doppler conditions. The proposed algorithm makes use of the feedback symbol mean value, $\mu_{x(k)}$. This value is used to: (a) compute and remove the ICI from the received data; and (b) to keep the LS estimator coefficients constant, as explained in the sequel.

It has been established in [26] that for normalized Doppler conditions of up to about 20%, channel time variations can be approximated by a piece-wise linear model with a constant slope over one OFDM symbol duration. Let $h^j_{avg}(l)$ and $\alpha^j(l)$ denote the time average and slope of the l^{th} channel tap at the j^{th} OFDM symbol, respectively. The linear model for the l^{th} channel tap at the i^{th} time instant within the j^{th} OFDM symbol, $h^j(i,l)$, therefore, can be written as

$$h^j(i,l) = h^j_{avg}(l) + \left(i - \frac{N-1}{2}\right)\alpha^j(l), \quad 0 \le i \le N-1, 0 \le l \le N_h - 1 \tag{14}$$

where $h^j_{avg}(l) = \frac{1}{N}\sum_{i=0}^{i=N-1} h^j(i,l)$. The value of $h^j_{avg}(l)$ is obtained from the IFFT of the channel estimates at the pilot subcarriers, as explained in the sequel. Knowing $h^j_{avg}(l)$, the slope $\alpha^j(l)$ can be computed easily from geometrical considerations [27].

Define $\alpha^j_{pre}(l) = \frac{h^j_{avg}(l) - h^{(j-1)}_{avg}(l)}{N}, (j > 0)$ and $\alpha^j_{post}(l) = \frac{h^{(j+1)}_{avg}(l) - h_{avg}{}^j(l)}{N}, j < j_{last}$, (Ref. Figure 3), where j_{last} is the last received OFDM symbol. Now,

$$\begin{aligned} \alpha^0(l) &= \alpha^0_{post}(l) \\ \alpha^j(l) &= \alpha^j_{pre}(l), i < \frac{N-1}{2} \\ &= \alpha^j_{post}(l), i \ge \frac{N-1}{2} \\ \alpha^{j_{last}}(l) &= \alpha^{j_{last}}_{pre}(l) \end{aligned} \tag{15}$$

We drop the superscript j in the development below.

As in the case of symbol estimation, approximating $x(d)$ by $\mu_{x(d)}$, we get, $y(k)$ from (5) as

$$\begin{aligned} y(k) &= \mathbf{H}(k,k)x(k) + \sum_{d=k-2L, d\neq k}^{k+2L} \mathbf{H}(k,d)x(d) + w(k) \\ &\approx \mathbf{H}(k,k)x(k) + \sum_{d=k-2L, d\neq k}^{k+2L} \mathbf{H}(k,d)\mu_{x(d)} + w(k) \end{aligned} \tag{16}$$

A piecewise linear channel model in the time domain, given by (14), leads to the following frequency domain channel coefficients:

$$\mathbf{H}(k,k) = \sum_{l=0}^{l=N_h-1} h_{avg}(l)e^{-j2\pi lk/N}, 0 \le k \le N-1 \tag{17}$$

and

$$\begin{aligned} \mathbf{H}(k,d) = \frac{1}{N}\sum_{l=0}^{l=N_h-1}\sum_{i=0}^{N-1}\left(i - \frac{N-1}{2}\right) \\ \times \alpha(l)e^{-j2\pi i(k-d)/N}e^{-j2\pi ld/N}, \\ 0 \le k \le N-1, -L \le (k-d) \le L, d \ne k. \end{aligned} \tag{18}$$

Define $\mathbf{h_{avg}} := [h_{avg}(0), h_{avg}(1), \cdots, h_{avg}(N_h-1)]^t$, $\boldsymbol{\alpha} := [\alpha(0), \alpha(1), \cdots, \alpha(N_h-1)]^t$, $\mathbf{b_k} = [1, e^{-j2\pi k/N}, \cdots, e^{-j2\pi k(N_h-1)/N}]^t$ and $C_{k-d} = \frac{-1}{1-e^{-j2\pi(k-d)/N}}$. (17) and (18) can now be written as

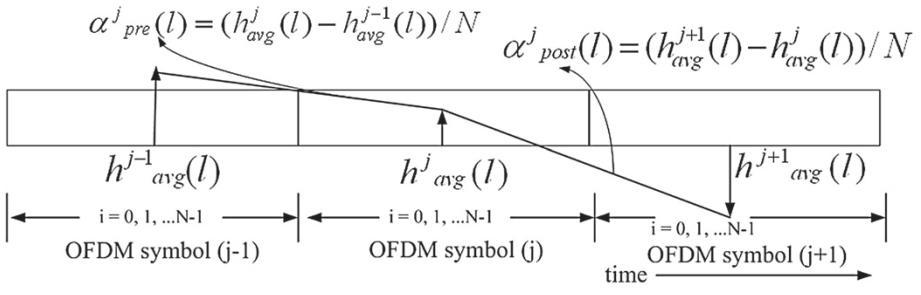

Figure 3 Slopes $\alpha^j_{pre}(l)$ and $\alpha^j_{post}(l)$ in channel estimation.

$$\mathbf{H}(k,k) = \mathbf{b_k}^t \cdot \mathbf{h_{avg}} \tag{19}$$

$$\mathbf{H}(k,d) = C_{k-d}\mathbf{b_d}^t\boldsymbol{\alpha} \tag{20}$$

In [5], $\mathbf{h_{avg}}$ and $\boldsymbol{\alpha}$ are jointly estimated from the same OFDM symbol. For a satisfactory performance of this scheme, pilot tones should be partitioned into equispaced groups on the FFT grid. This limits the use of this scheme in systems such as DVB [22] or *IEEE*802.16 [21], where an equispaced pilot pattern (with no grouping) is deployed.

In the proposed scheme, as in the case of equalization, we first remove the ICI from the received data, using the channel estimates and feedback symbol mean values obtained from the previous iteration. The modified system matrix is diagonal, with the elements given in (19). An equispaced pilot pattern is best suited for $\mathbf{h_{avg}}$ estimation in the modified system. This enables the proposed scheme not to have the limitation cited above, thus making it especially suitable for practical systems. A progressively improving estimate of $\mathbf{h_{avg}}$ is computed as explained below. An improved estimate of $\boldsymbol{\alpha}$ can be obtained from the new $\mathbf{h_{avg}}$ (15). Note from (19) and (20) that the diagonal elements of $\mathbf{H}$ can be computed from $\mathbf{h_{avg}}$, whereas the off-diagonal elements of $\mathbf{H}$ (which cause ICI) can be computed from $\boldsymbol{\alpha}$.

The ICI-removed received data, $y'(k) \approx y(k) - \sum_{d=k-2L,d\neq k}^{k+2L} C_{k-d}\mathbf{b_d}^t\boldsymbol{\alpha}\mu_{x(d)}$, can be written in vector form as

$$\mathbf{y}' = diag(\boldsymbol{\mu}_x)\cdot(\mathbf{A}\mathbf{h_{avg}}) + \mathbf{w} \tag{21}$$

where the $N \times N_h$ matrix $\mathbf{A}$ is given by $\mathbf{A} = [\mathbf{b_0}, \mathbf{b_1}, \cdots, \mathbf{b_{N-1}}]^t$. Premultiplying (21) with $(diag(\boldsymbol{\mu}_x))^{-1}$, we get

$$\check{\mathbf{y}} = \mathbf{A}\mathbf{h_{avg}} + \check{\mathbf{w}} \tag{22}$$

where $\check{\mathbf{y}} = [\frac{y'(0)}{\mu(0)}, \cdots, \frac{y'(N-1)}{\mu(N-1)}]^t$ and $\check{\mathbf{w}} = [\frac{w(0)}{\mu(0)}, \cdots, \frac{w(N-1)}{\mu(N-1)}]^t$. The LS estimate of $\mathbf{h_{avg}}$ can be obtained from (22) as

$$\mathbf{h_{avg}} = (\mathbf{A}^H\mathbf{A})^{-1}\mathbf{A}^H\check{\mathbf{y}}. \tag{23}$$

Observe that the LS coefficients are constants and can be precomputed and stored thus avoiding costly matrix multiplication and inverse operations and making this estimation scheme low in complexity. We thus estimate each $h_{avg}(l)$ with only a vector multiplication. Our aim is to generate an initial estimate of $\mathbf{h_{avg}}$ and $\boldsymbol{\alpha}$ using pilots and subsequently refine them in every iteration using the feedback mean values. Assume that there are P pilot tones and they are placed at subcarriers $\mathbb{P} = \{p(1), \cdots, p(P)\}$. Transmit symbols at pilot tones $x_p(1), x_p(2), \cdots, x_p(P)$ are known at the receiver. The initial estimate of $\mathbf{h_{avg}}$ is computed using the LS solution

$$\mathbf{h_{avg}} = (\mathbf{A_p}^H\mathbf{A_p})^{-1}\mathbf{A_p}^H\check{\mathbf{y}}_p \tag{24}$$

where $\mathbf{A_p} = [\mathbf{b_{p(1)}}, \mathbf{b_{p(2)}}, \cdots, \mathbf{b_{p(P)}}]^t$ and $\check{\mathbf{y}}_p = [\check{y}_{p(1)}, \check{y}_{p(2)}, \cdots, \check{y}_{p(P)}]^t$. The LS estimate using (24) does not, however, give accurate results when $P < N_h$. For subsequent iterations, compute $\mathbf{h_{avg}}$ by setting $\check{y}(k) = 0$ or $\check{y}(k) = y'(k)/\mu_x(k)$ in (23), based on a threshold value of the conditional feedback variance $\nu_x(k)$ (13) obtained from the decoder at the end of the previous iteration. The threshold should be small enough so that $\mu_x(k)$ is close to the actual symbol value. Since $\nu_x(k)$ is small, hard slicing $\mu_{x(k)}$ to the nearest $x(k)$ is also found to be effective as the error propagation is largely absent. $\boldsymbol{\alpha}$ is computed from (15). As $\nu_x(k) \to 0$, $\mu_x(k) \to x(k)$. Thus, the channel estimate progressively improves as the iterations proceed. Since $N_h \leq N_p$, LS estimate can also be computed from a submatrix $\mathbf{A_{CP}}$ of $\mathbf{A}$, such that $\mathbf{A_{CP}}$ is at least $N_p \times N$ in size and the chosen N_p rows should contain the rows corresponding to that of pilots in the system. A distinct advantage of this iterative estimation method is that it does not set the lower limit,($N_h \leq P$), on the number of pilot subcarriers, as most of the data carriers act as pilots from the second iteration onwards.

Operation of the proposed IR algorithm is enumerated in the next subsection.

The proposed IR with SIC-MAP

1. Choose the maximum number of iterations.
2. For each iteration and for each frequency bin k, compute channel estimate $\mathbf{H_k}$.
   (a) Compute $\mathbf{h_{avg}}$ (23) or (24) as the case may be. For the first iteration, use $\mu_x(k) = 0$; otherwise, use $\mu_x(k)$ from steps 11, 12. For each frequency bin k, compute $\mathbf{H}(k,k)$ (19).
   (b) Compute $\boldsymbol{\alpha}$ (15). Compute $\mathbf{H}(k,d)$ for all $d \neq k$ $(k-2L \leq d \leq k+2L)$ (20).
3. Compute $\tilde{\mathbf{y}}_\mathbf{k}$ from $\mathbf{y}$ (5), (8). For the first iteration, use $\mu_x(k) = 0$; otherwise, use $\mu_x(k)$ from steps 11,12.
4. Perform symbol de-interleaving.
5. Compute $LLR_{ext}(c(\cdot))$ (10), (11).
6. Perform bit de-interleaving.
7. Compute $LLR_{\text{app}}(b(n))$ using BCJR/SOVA.
8. If $LLR_{\text{app}}(b(n))$s are sufficiently converged or the maximum number of iterations is reached, hard-slice $LLR_{\text{app}}(b(n))$. Output the information bits $\hat{a}(n)$ and stop the iterations; otherwise,
9. Compute $LLR'_{\text{ext}}(b(n))$.
10. Perform bit interleaving.
11. Compute $\mu'_s(k)$ (12).
12. Perform symbol interleaving.
13. Go to step 2.

Computational complexity analysis

In this section, the computational complexity of SIC-MAP is compared to the iterative equalization schemes MMSE-TE-OND2 [18] and TE-BLK2 [19]. The complexity of the non-iterative MMSE scheme [27] that is popularly used in practical receivers, referred to as MMSE-OND2 in this article, is also computed. MMSE-OND2 is based on a section of $\mathbf{H}$ ($\mathbf{H_k}$ in Figure 2(right)), given in (6). MMSE-OND2 schemes, turbo or not, involve the inversion of a matrix of size D. Matrix inversion generally has cubic complexity. However, it has been shown that MMSE-OND2 or MMSE-TE-OND2 can be performed with approximately $O(N \cdot D^2)$ operations [28]. Table 1 tabulates the total number of arithmetic operations $(\times, \div)$ required at the receiver for different schemes. Computations involved in BCJR are identical across all these schemes and, therefore, are not considered. (The cost of adders is significantly lower than that of multipliers. *tanh* operation can be performed using a small lookup table. These two operations are, thus, not tabulated in Table 1. Although not differentiated here, the cost of a divider, in practice, is higher than that of a multiplier.)

For a typical set of parameters ($L = 1$), it is clear from Table 1 that TE-BLK2 and MMSE-TE-OND2 require approximately 3.3 and 4.5 times more computations than SIC-MAP per iteration, while the channel estimation efforts are the same. The noniterative scheme, MMSE-OND2, requires 3.6 times more computations than SIC-MAP per iteration.

Numerical results and discussion

In this section, we present the results of numerical simulations of the proposed IR over doubly selective channels. This section has two parts. In the first part, we evaluate SIC-MAP by comparing its performance with two other iterative schemes described in **Computational complexity analysis** section. For this purpose, we assume that CSI is known at the receiver. We consider an OFDM system with $N = 256$, $N_h = 30$ and $N_p = N/4$. A 1/2 rate convolutional code with generator polynomial $(7, 5)$ is used. Symbols are QPSK modulated with unit variance. AWGN has a circular variance of $(E_b/N_0)^{-1}$. Both bit and symbol interleaving are performed with S-random interleavers [29], with $S = 22$ and $S = 5$, respectively. Each channel path is Rayleigh fading, characterized by Jakes' Doppler Spectrum (exponentially decaying power delay profile), with a frequency spread of $f_d = 900Hz$. With the DVB-T sampling rate of $T_s^{-1} = 9.14MHz$, this corresponds to a normalized Doppler spread of 20% of the subcarrier spacing.

Figure 4 shows the BER performance of the three schemes used in our study. Although windowing employed in [18,19] can improve the performance in all three schemes, no windowing is employed in our study, as it increases the computation burden significantly. SIC-MAP performs poorly in the first iteration, as no interference is canceled before computing the LLRs. The incremental BER gain, however, between the first and second iterations of SIC-MAP is very significant. Therefore, MMSE-TE-OND2 and SIC-MAP perform more or less identically within three iterations. Note that the computational complexity of SIC-MAP is roughly only 22% that of MMSE-TE-OND2. It was shown in [19] that the performance of TE-BLK2 is superior to MMSE-TE-OND2 [18]. This can be seen from Figure 4. However, the performance difference is not significant in a system where error correction coding (convolutional coding, in this case) is incorporated, as is the case with most practical receivers. A SIC-MAP scheme can be implemented with only a third of the computations that are required for TE-BLK2. (Entries corresponding to TE-BLK2 in Table 1 are obtained from [19].) BER performance of the noniterative MMSE-OND2 [27] is that corresponding to the first iteration of MMSE-TE-OND2. From Table 1, note that the complexity of MMSE-OND2 is approximately 3.6 times higher than that of SIC-MAP. From Figure 4 observe that SIC-MAP converges sufficiently in three iterations and outperforms MMSE-OND2 significantly. Thus, we conclude that SIC-MAP has all the performance benefits of any iterative scheme, yet its total computational complexity is far less even than that of a commonly used noniterative scheme, namely MMSE-OND2.

Table 1 Complexity comparison—channel equalization

	TE-BLK2 per sample per iter.	MMSE-OND2 per sample	MMSE-TE-OND2 per sample per iter.	SIC-MAP per sample per iter.
Total $\times$	$12L^2 + 24L + 17$	$(2L + 1)(18L + 4)$	$(2L + 1)(20L + 7) + 2$	$2(2L + 1)^2 + 1$
Total $\div$	$2L + 7$	$2L$	$(2L + 1)$	–
Total Oper.	$12L^2 + 26L + 24$	$2L + (2L + 1)(18L + 4)$	$(2L + 1) + (2L + 1)(20L + 7) + 2$	$2(2L + 1)^2 + 1$
Normalized Complexity (L=1)	3.3	3.6	4.5	1

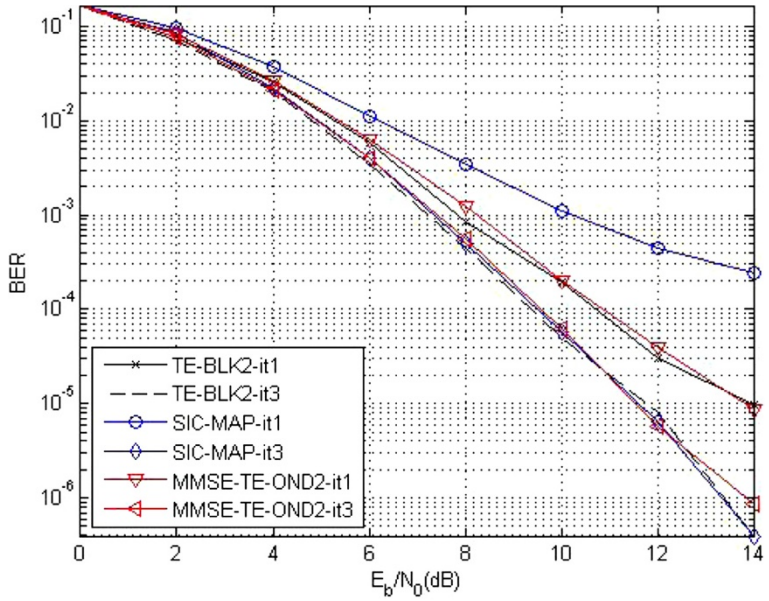

Figure 4 BER comparison of different equalization schemes ($f_d T_s N = 0.2, N = 256, L = 1$, MMSE-TE-OND2 $\#iter = 1, 3$, SIC-MAP $\#iter = 1, 3$, TE-BLK2 $\#iter = 1, 3, N_h = 30$).

If we set $L = 3$ for SIC-MAP but $L = 1$ for the other two schemes, all three schemes will approximately have the same computational cost. The performance of such a system is given in Figure 5. As can be seen, for the same computational cost, SIC-MAP clearly outperforms MMSE-TE-OND2 and MMSE-TE-BLK2.

In the second part, we examine the performance of these receivers when employing the low-complexity channel estimation scheme described in **Channel estimation** section.

In Figure 6, performance of SIC-MAP, MMSE-TE-OND2- and MMSE-OND2-based receivers that employ the aforementioned channel estimation scheme is compared. These receivers have 32 equispaced pilots per OFDM symbol. The system has $N_h = 30$ and a normalized Doppler of 20%. Performance of the IRs, as can be

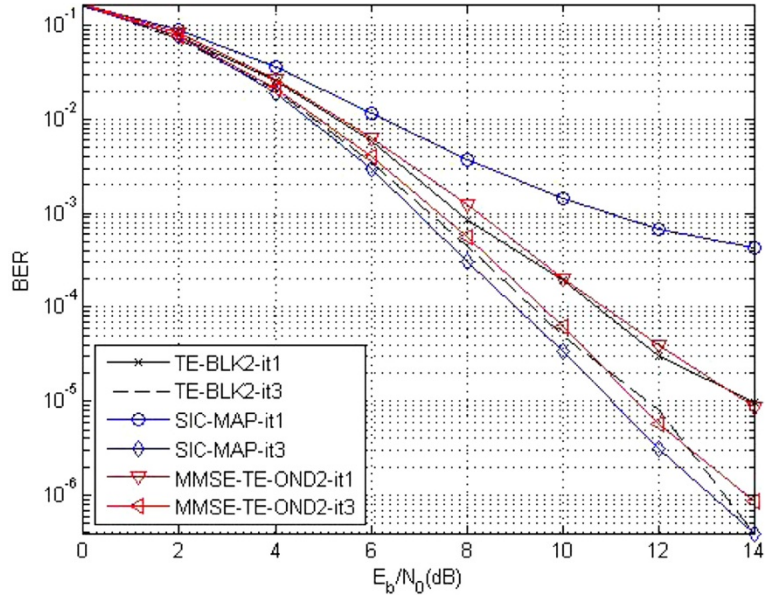

Figure 5 BER comparison when more off diagonals are incorporated in SIC-MAP to match the complexity to MMSE-TE-OND2 ($f_d T_s N = 0.2, N = 256, L = 1$ for MMSE-TE-OND2 $\#iter = 1, 3$ and TE-BLK2 $\#iter = 1, 3$, but $L = 3$ for SIC-MAP $\#iter = 1, 3, N_h = 30$).

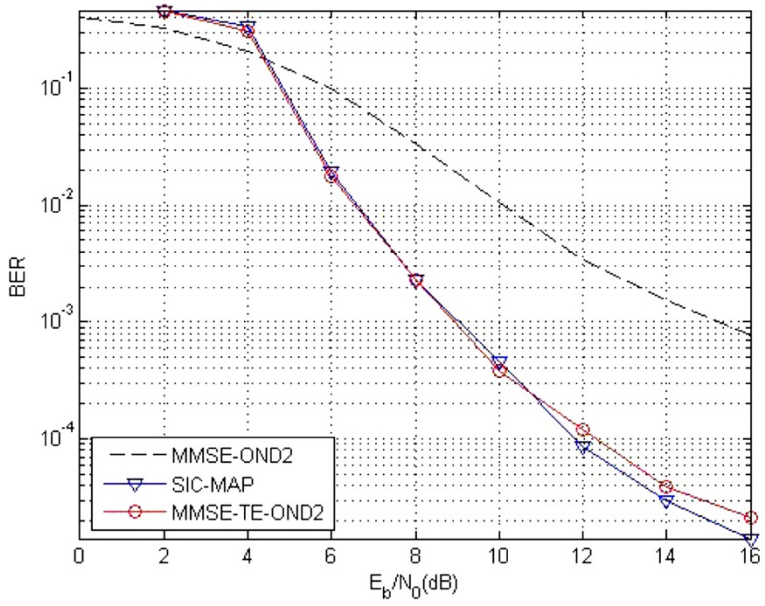

Figure 6 BER comparison of different IRs with channel estimation ($N_h \leq P$). ($f_dT_sN = 0.2$, $N = 256$, $L = 1$, $\#iter = 3$, $P = 32$, $N_h = 30$).

seen from the figure, is significantly better than the noniterative receiver at moderate to high SNR region. Both the iterative schemes perform nearly identically, as expected.

Figure 7 depicts the behavior of the estimation scheme when the number of channel taps ($N_h = 40$) is more than the number of pilots ($N_p = 32$). Comparing Figures 6 and 7, it is clear that the iterative schemes perform identically in both scenarios ($N_h \leq P$ and $N_h > P$) at SNRs of practical interest, whereas the noniterative scheme performance is considerably poorer in the latter case.

Conclusion

We have proposed a low-complexity IR employing successive interference cancelation to mitigate the effects of ICI in mobile OFDM systems. The proposed scheme, SIC-MAP, while having nearly identical performance to MMSE-TE-OND2 and TE-BLK2, can be implemented with only 22% and 30%, respectively, of their computational burden. It was also found that performance and implementation complexity of SIC-MAP can effectively be traded for one another. A low-cost iterative LS channel

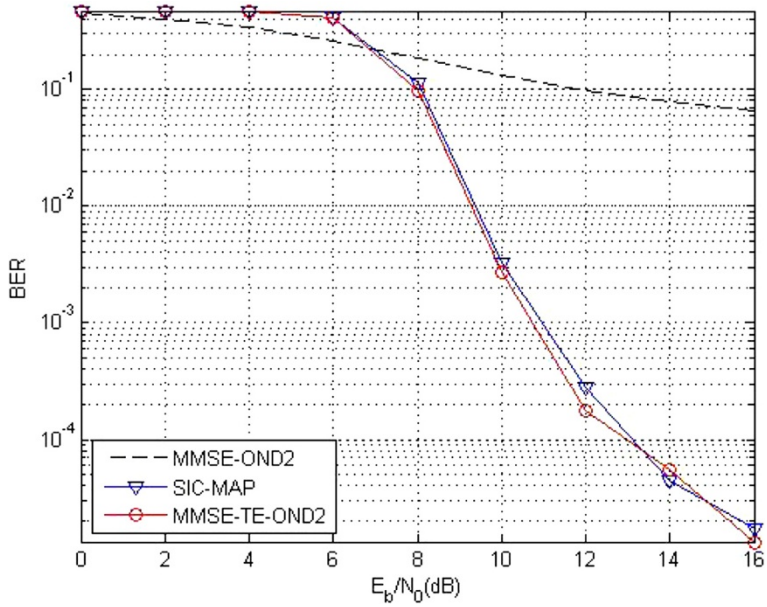

Figure 7 BER comparison of different IRs with channel estimation ($N_h > P$). ($f_dT_sN = 0.2$, $N = 256$, $L = 1$, $\#iter = 3$, $P = 32$, $N_h = 40$).

Table 2 QPSK alphabet

	1	2	3	4
$(m0, m1)$	$(0,0)$	$(1,0)$	$(0,1)$	$(1,1)$
η_i	$\frac{1+j1}{\sqrt{2}}$	$\frac{-1+j1}{\sqrt{2}}$	$\frac{1-j1}{\sqrt{2}}$	$\frac{-1-j1}{\sqrt{2}}$

estimation scheme, suitable for practical receivers, is also proposed. Besides low complexity, another advantage of the iterative channel estimation scheme is that, unlike pilot-only based LS schemes, it works satisfactorily for systems that have a higher number of channel taps than pilot subcarriers, a phenomenon that is commonly encountered in DVB systems deployed in single frequency networks.

Appendix

Derivation of (10)

Ref. to Table 2 for the QPSK symbol alphabet definition.

$$LLR_{ext}(c(2k)) = ln\frac{p(\tilde{\mathbf{y}}_k/x(k)=\eta_1)P(0) + p(\tilde{\mathbf{y}}_k/x(k)=\eta_3)P(1)}{p(\tilde{\mathbf{y}}_k/x(k)=\eta_2)P(0) + p(\tilde{\mathbf{y}}_k/x(k)=\eta_4)P(1)} \tag{25}$$

Here

$$\begin{aligned} p(\tilde{\mathbf{y}}_k/x(k)=\eta_1) &= exp(-\frac{(\tilde{\mathbf{y}}_k - \mathbf{h_k}\eta_1)^H(\tilde{\mathbf{y}}_k - \mathbf{h_k}\eta_1)}{2\sigma^2}) \\ &= exp(\frac{-1}{2\sigma^2}(a1 + a2 - 2Re(\mathbf{y_k}^H\mathbf{h_k}\eta_1)) \end{aligned} \tag{26}$$

where $a1 = \mathbf{y_k}^H\mathbf{y_k}$ and $a2 = (\mathbf{h_k}\eta_1)^H(\mathbf{h_k}\eta_1)$. Note that, for QPSK $(\mathbf{h_k}\eta_1)^H(\mathbf{h_k}\eta_1) = (\mathbf{h_k}\eta_2)^H(\mathbf{h_k}\eta_2) = (\mathbf{h_k}\eta_3)^H(\mathbf{h_k}\eta_3) = (\mathbf{h_k}\eta_4)^H(\mathbf{h_k}\eta_4)$. Substituting for all the terms from (26) in (25), defining $z := \tilde{\mathbf{y}}_k^H\mathbf{h_k}$ and removing the common terms, we get,

$$\begin{aligned} &LLR_{ext}(c(2k)) \\ &= ln\frac{exp(Re(z\eta_1)/\sigma^2)P(0) + exp(Re(z\eta_3)/\sigma^2)P(1)}{exp(Re(z\eta_2)/\sigma^2)P(0) + exp(Re(z\eta_4)/\sigma^2)P(1)} \\ &= ln\frac{exp(\sqrt{2}Re(z(1+j))/\sigma^2)P(0)+exp(Re(z(1-j))/\sigma^2)P(1)}{exp(\sqrt{2}Re(z(-1+j))/\sigma^2)P(0)+exp(Re(z(-1-j))/\sigma^2)P(1)} \\ &= ln\frac{exp(\sqrt{2}(Re(z)-Im(z))/\sigma^2)P(0)+exp(\sqrt{2}(Re(z)+Im(z))/\sigma^2)P(1)}{exp(\sqrt{2}(-Re(z)-Im(z))/\sigma^2)P(0)+exp(\sqrt{2}(-Re(z)+Im(z))/\sigma^2)P(1)} \\ &= ln\left(\frac{exp(\frac{\sqrt{2}}{\sigma^2}Re(z))}{exp(\frac{-\sqrt{2}}{\sigma^2}Re(z))}\right) \\ &= \frac{\sqrt{8}Re(\tilde{\mathbf{y}}_k^H\mathbf{h_k})}{\sigma^2}. \end{aligned} \tag{27}$$

Similarly we get $LLR_{ext}(c(2k+1)) = \frac{\sqrt{8}Im(\tilde{\mathbf{y}}_k^H\mathbf{h_k})}{\sigma^2}$

Competing interests
The authors declare that they have no competing interests.

Received: 7 September 2011 Accepted: 24 May 2012
Published: 1 August 2012

References

1. JPMG Linnartz, A Gorokhov, New equalization approach for OFDM over dispersive and rapidly time varying channel. Proc. IEEE Int. Symp. Pers. Indoor Mob. Radio Commun. **2**, 1375–1379 (2000)
2. P Baracca, S Tomasin, L Vangelista, N Benvenuto, A Morello, Per sub-block equalization of very long OFDM blocks in mobile communications. IEEE Trans. Commun. **59**, 363–368 (2011)
3. S Tomasin, A Gorokhov, H Yang, J-P Linnartz, Iterative interference cancellation and channel estimation for mobile OFDM. IEEE Trans. Wirel. Commun. **4**(1), 238–245 (2005)
4. QGL Ping, D Huang, A low complexity iterative channel estimation and detection technique for doubly selective channels. IEEE Trans. Wirel. Commun. **8**(1), 4340–4349 (2009)
5. S Chen, T Yao, Intercarrier interference suppression and channel estimation for OFDM systems in time-varying frequency-selective fading channels. IEEE Trans. Consumer Electron. **50**, 429–435 (2004)
6. H Lee, B Lee, I Lee, Iterative detection and decoding with an improved V-BLAST for MIMO-OFDM systems. IEEE J. Select. Areas Commun. **24**, 504–513 (2006)
7. SU Hwang, JH Lee, J Seo, Low complexity iterative ICI cancellation and equalization for OFDM systems over doubly selective channels. IEEE Trans. Broadcast. **55**(1), 132–139 (2009)
8. RC de Lamare, R Sampaio-Neto, Minimum mean-squared error iterative minimum mean-squared error iterative successive parallel arbitrated decision feedback detectors for DS-CDMA systems. IEEE Trans. Commun. **56**(5), 778–789 (2008)
9. C Douillard, M Jezequell, C Berrou, A Picart, P Didier, A Glavieux, Iterative correction of inter-symbol interference: Turbo equalization. Eur. Trans. Telecommun. **6**, 507–511 (1995)
10. X Wang, HV Poor, Iterative (turbo) soft interference cancellation and decoding for coded CDMA. IEEE Trans. Commun. **47**, 1046–1061 (1999)
11. M Tüchler, A Singer, R Kotter, Minimum mean squared error (MMSE) equalization using a priori information. IEEE Trans. Sig. Process. **50**, 673–683 (2002)
12. J Huang, S Zhou, J Huang, CR Berger, P Willett, Progressive inter-carrier interference equalization for OFDM transmission over time-varying underwater acoustic channels. IEEE J. Select. Topics Sig. Process. **5**, 1524–1536 (2011)
13. E Panayirci, H Dogan, HV Poor, Low-complexity MAP-based successive data detection for coded ofdm systems over highly mobile wireless channels. IEEE Trans. Vehicul. Technol. **60**, 2849–2857 (2011)
14. JW Choi, AC Singer, J Lee, NI Cho, Improved linear soft-input soft-output detection via soft feedback successive interference cancellation. IEEE Trans. Commun. **58**, 986–996 (2010)
15. AF Molisch, M Toeltsch, S Vermani, Iterative methods for cancellation of intercarrier interference in OFDM systems. IEEE Trans. Vehicul. Technol. **56**(4), 2158–2167 (2007)
16. S Jiang, L Ping, H Sun, CS Leung, Modified LMMSE turbo equalization. IEEE Commun. Lett. **8**, 173–176 (2004)
17. S Ahmed, M Sellathurai, JA Chambers, Low complexity iterative method of equalization for OFDM in doubly selective channels. in *Proceedings of Asilomar Conference on Signals, Systems and Computers,* (2005), pp. 687–691
18. P Schniter, Low-complexity equalization of OFDM in doubly selective channels. IEEE Trans. Sig. Process. **52**(4), 1002–1011 (2004)
19. K Fang, L Rugini, G Leus, Low-complexity block turbo equalization for OFDM systems in time—varying channels. IEEE Trans. Sig. Process. **56**, 5555–5566 (2008)
20. WG Jeon, KH Chang, YS Cho, An equalization technique for orthogonal frequency-division multiplexing systems in time-variant multipath channels. IEEE Trans. Commun. **47**, 27–31 (1999)
21. Air Interface for Fixed Broadband Wireless Access Systems: Part A: Systems Between 2–11GHz. *IEEE Stand. 802.16, 01/01r1* (2001)

22. Digital Video Broadcasting (DVB): Framing Structure, Channel Coding and Modulation for Digital Terrestrial Television. *ETSI Standard. ETS 300 744* (1999)
23. O Edfors, M Sandell, J-J van de Beek, SK Wilson, PO Börjesson, OFDM channel estimation by singular value decomposition. IEEE Trans. Commun. **46**(7), 931–939 (1998)
24. S Lin, DJ Costello, *Error Control Coding* (Prentice Hall, London, 2004)
25. WC Jakes, *Microwave Mobile Communications* (Wiley, New York, 1974)
26. Y Mostofi, DC Cox, ICI mitigation for pilot-aided OFDM Mobile systems. IEEE Trans. Wirel. Commun. **4**(2), 765–774 (2005)
27. S Lu, B Narasimhan, N Al-Dhahir, A novel SFBC-OFDM scheme for doubly selective channels. **58**(5), 2573–2578 (2009)
28. L Hong, *Frequency Domain Equalization of Single Carrier Transmissions Over Doubly Selective Channels*. PhD thesis, The Ohio State University, (2007)
29. C Heegard, S Wicker, *Turbo Coding* (Kluwer, Boston, 1999)

doi:10.1186/1687-6180-2012-166
Cite this article as: Namboodiri *et al.*: **Low-complexity iterative receiver design for mobile OFDM systems.** *EURASIP Journal on Advances in Signal Processing* 2012 **2012**:166.